Polycrystal Scattering Topography, Scattering Tomography and their Perspective Fields of Application

Yasuharu Yoneda
Department of Applied Physics, Kyushu University, Higashi-ku, 812 Fukuoka-shi, Japan

Yoshinori Chikaura
Department of Physics, Kyushu Institute of Technology, Sensui-cho, Tobata-ku, 804 Kitakyushu-shi, Japan

Z. Naturforsch. **37a**, 412–418 (1982); received December 18, 1981

Dedicated to Professor Dr. G. Hildebrandt, Fritz-Haber-Institut der Max-Planck-Gesellschaft, Berlin, to celebrate his sixtieth birthday

A concept of X-ray topography for polycrystalline materials has been proposed. In this method X-rays scattered from a specimen produce the image. Various techniques for this kind of topography are described and their characteristic features are pointed out; some of these techniques offer the possibility to make tomographic observations.

The new topographic method has been applied to the observation of commercially used aluminium sheet and of wood (cedar). The discussion is extended to mechanisms of the image formation and the perspective fields of application.

1. Introduction

A new kind of X-ray topography has been devised to observe polycrystalline, amorphous or biological materials [1, 2]. In this method X-rays scattered from a polycrystal produce a topographical image. We call this Polycrystal Scattering Topography (PST). PST enables, in principle, to make tomographic observations. Taking advantage of this function we have extended the basic principle to X-ray tomography, particularly to medical diagnosis or biological studies [3]. This method is named Scattering Tomography (ST). Independent of us, Born and Schwarzbauer [4, 5] have also contributed to the development of the concept of PST. They have devised two techniques of PST using a Soller slit or a diaphragm to observe e.g. textures of aluminium coins; they call their technique texture topography.

The aim of the present paper is to compare the characteristic features of our PST, our ST and Born's original one, and to discuss the perspective fields of application. Selected examples of PST observations are also described in order to demonstrate the feasibility of the new imaging methods. Finally we propose an equipment of PST with synchrotron radiation.

Reprint requests to Prof. Dr. Y. Chikaura, Department of Physics, Kyushu Institute of Technology, Sensui-cho, Tobata-ku, 804 Kitakyushu-shi, Japan.

2. Principle and Apparatus

2.1. Principle

The basic principle of PST consists in mapping the X-ray intensity scattered elastically or inelastically from a specimen. We choose the most proper kind of X-rays to observe the spatial distribution of a physical quantity such as crystal structure, fluorescence (absorption edge), Compton scattering, texture, crystallite size or internal stress. Taking the texture observation in metal plates for example, Debye-Scherrer diffracted X-rays are found to be most suitable for it. When observing material-distribution, we may take advantage of the fluorescent X-rays from the specimen.

In order to obtain significant images of polycrystalline specimens, collimators (Soller slits or crystal collimators) and specimen scanning mechanisms are employed for guaranteeing one to one geometrical correspondence between the specimen and the image on the X-ray emulsion film or cathode ray tube. Several techniques fulfilling this condition which have been proposed by the present authors and Born and Schwarzbauer are compared with the other modified techniques in the next section.

0340-4811 / 82 / 0500-0412 $ 01.30/0. — Please order a reprint rather than making your own copy.

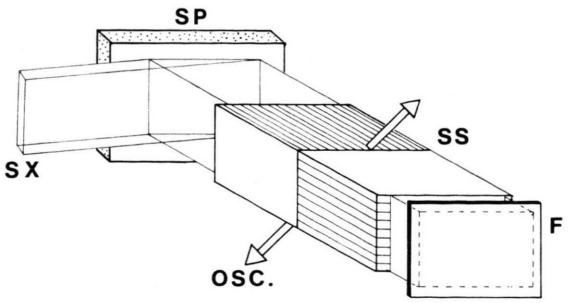

Fig. 1. Schematic principle of the cross Soller slit method. SX: extended source of X-rays, SP: specimen, SS: Soller slit, F: emulsion film, OSC: oscillating direction.

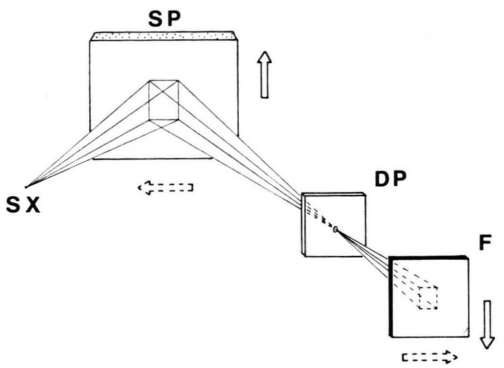

Fig. 2. Schematic principle of the diaphragm method [5]. DP: diaphragm, SX: point source of X-rays. Arrows with solid line and broken line indicate two-dimensional opposit scanning of the specimen SP and the emulsion film F.

2.2. Apparatus

(a) Cross Soller Slit Method

Figure 1 shows a schematic principle of this technique in the reflection case [1]. The geometry is characterized by two Soller slits rotated by 90° with respect to each other, and an oscillating mechanism along a direction between the normals of the two Soller slit planes as indicated in Figure 1. The oscillation is performed to eliminate the shadows of the slit materials. A technique for making a Soller slit with high parallelism of the order of 10^{-3} rad. is briefly described in the section (d). With such Soller slits we attain the resolution of 0.2—0.3 mm. One of the advantages of this system is simplicity of the equipment; we need no mechanism for scanning the specimen.

(b) Diaphragm Method [4] (Born's Method)

The whole geometry of the diaphragm technique by Born and Schwarzbauer [4] is shown schematically in Figure 2. In this geometry a diaphragm DP and the place of a point X-ray source are arranged on the reflection circle. Therefore the spatial resolution is determined mainly by the sizes of the diaphragm and the point source of X-rays. Arrangement of the diaphragm at the focus of the reflected X-rays also gives a serious influence on the resolution. If we employ a diaphragm with a diameter of 0.1 mm and an apparent point source of X-rays of the same order in size (real focus size of 0.1 mm × 1 mm, take-off angle of 6°), we attain a resolution of 0.1 mm provided that the geometrical arrangement of the experimental set-up is performed within a preciseness of 0.1 mm.

A remarkable difference of this geometry in relation to the first PST set-up (Fig. 1) is the inverse position of image and object, whereas the cross Soller slit arrangement gives normal projection of the specimen. The merit of this technique is the geometrical simplicity; if we can tolerate a smaller field of vision (say, 3 mm × 3 mm in size), the PST image can be obtained without a scanning mechanism of the specimen. However, when we enlarge the area of imaging, the specimen and the film have to be scanned parallel to each other but in opposite directions both in the plane of diffraction and perpendicular to it. The two-dimensional opposite scanning of the specimen and the emulsion film needs a somewhat complicated mechanism. This is one of the difficulties involved in the diaphragm technique.

(c) Parallel Solar Slit Method

A modified method of the diaphragm technique is shown schematically in Figure 3; the geometrical characteristic is the use of an extended source of

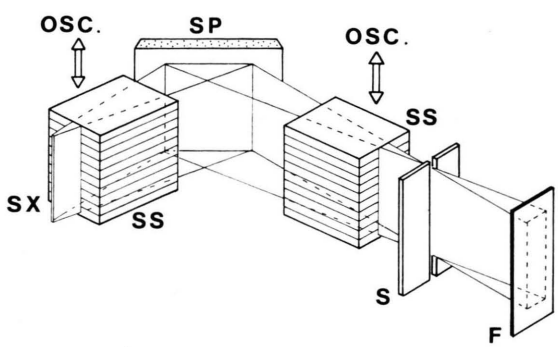

Fig. 3. Schematic principle of the parallel Soller slit method. OSC: oscillation of the Soller slits SS, S: slit, SX: line source of X-rays.

X-rays and of two Soller slits placed along incident and scattered beams, respectively. The system needs no scanning mechanism of the specimen parallel to the direction of the extended source of X-rays. Like the diaphragm method, the parallel Soller slit method is suitable for surface topography of polycrystals. It is possible to attain a resolution of the same order as that of the diaphragm technique.

(d) Soller Slit Oscillating Method

Figure 4 (a) shows a schematic principle of this technique in the transmission case. This system consists of a horizontal scanning mechanism for the specimen and emulsion film, a vertical oscillating mechanism for a Soller slit (SS) and two stationary slits S_1, S_2. The Soller slit with parallelism of 9×10^{-3} rad. can be made of steel razor blades (each size; 43 mm × 21 mm × 0.1 mm). The vertical oscillation is performed to smear out the shadows of the slit materials. When using Debye-Scherrer diffraction from polycrystalline metals and a normal X-ray tube operated at 40 kV/20 mA, and allowing as a tolerable exposure time several ten of hours, a spatial resolution of the order of 0.1 mm can be easily attained by properly adjusting the slits S_1 and S_2. This system provides two main advantages: it enables us to make three-dimensional observations, and the whole view of the PST image is produced with the same reflection condition. A reflection vector can be defined in one frame of the PST image. Therefore this method is particularly suitable for a study of texture distribution because almost all textured materials reflect X-rays in a limited azimuthal angular range on a Debye-Scherrer ring.

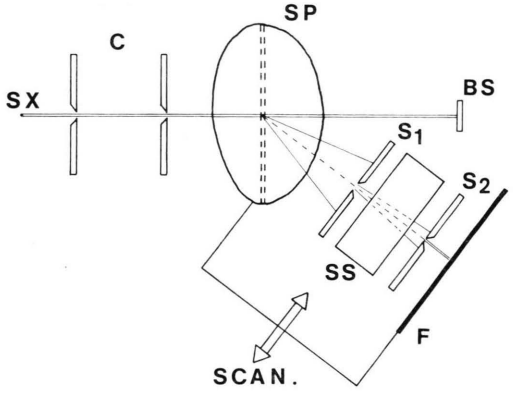

Fig. 4. Schematic principle of the Soller slit oscillating method. SX: point source of X-rays, S_1 and S_2: slits, BS: beam stopper, C: collimator of the incident beam, SS: Soller slit, oscillating perpendicularly to the plane of the figure. The specimen SP and the film F are scanned simultaneously (SCAN).

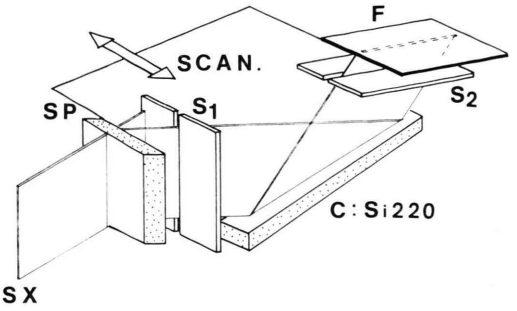

Fig. 5. Schematic principle of crystal collimator-slit combination method. C: crystal collimator, e.g. silicon, 220 reflection. SCAN: simultaneous scan of SP and F.

(e) Crytal Collimator-slit Combination Method

The Soller slit in the PST method described in the section (d) can be replaced by a crystal collimator, as shown in Figure 5. A dislocation-free crystal such as a silicon single crystal has to be used. Although the required exposure time becomes three to five times longer compared to the Soller slit oscillating method, this system has the peerless merit of a high resolution and high image contrast. The other characteristics of this technique are similar to those of the Soller slit oscillating method. Accordingly this method can be used for the precise observation of textured materials with a strong X-ray source such as a rotating anode.

(f) X-Y Scanning Method

The PST methods described in the sections (a) to (e) have, more or less, the serious disadvantage of long exposure time; several hours to several ten hours under X-ray condition 40 kV/20 mA (a normal sealed-off X-ray tube) are required depending on the wanted resolution and the diffraction geometry. In order to eliminate this demerit we adopt an electronic imaging procedure and a two-dimensional scanning mechanism of the specimen synchronized with the electron scanning in a cathode ray tube (CRT). The whole system in the transmission case is schematically shown in Figure 6. A pencil beam of X-rays enters the specimen. X-rays scattered from one point go through a cone-shaped slit to a detector D. The cone slit normally consists of two

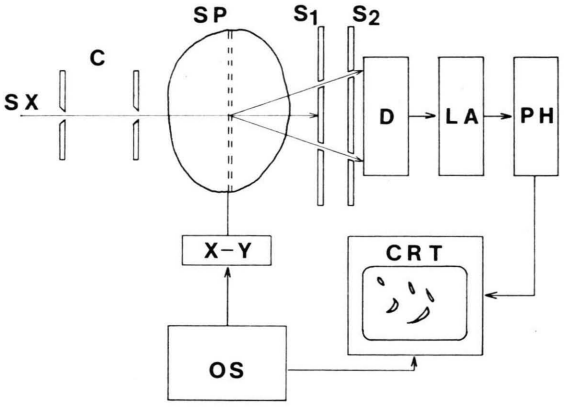

Fig. 6. Schematic principle of the X-Y scanning method. D: detector, LA: linear amplifier, PH: pulse height analyser, CRT: cathode ray tube, XY: two-dimensional scanning mechanism, C: collimating slit of the incident pencil beam, SX: point source of X-rays.

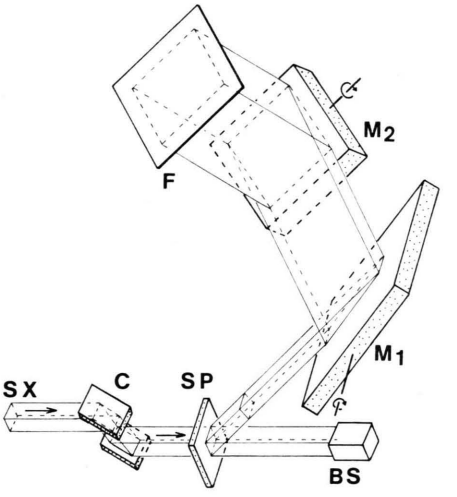

Fig. 7. Schematic principle of the PST equipment with synchrotron radiation. SX: synchrotron radiation, C: double-crystal monochromator made of a crystal block. M_1 and M_2: two-dimensional collimators (with asymmetric reflections, producing an enlarged image) for the X-rays scattered from the specimen SP. F: film emulsion or position sensitive proportional counter. BS: beam stop.

circular slits. A deformed cone slit can also be used when observing anisotropic materials such as heavily deformed metals, wood or other biological materials. The detector D, linear amplifier LA and pulse-height analyser PH modulate the beam intensity in the CRT. The exposure time for this system is typically 10 to 30 min under X-ray condition 40 kV/20 mA. Although the spatial resolution depends on the preciseness of the arrangement, we have easily obtained a resolution better than 0.1 mm.

The system can be modified to a multi-color television system by employing a solid state detector, multi-channel analyser and multi-color CRT [6]. Since this system enables us to make tomographic observations, we call this scattering tomography when the tomographic function should be emphasized, particularly in the field of medical diagnosis [3].

(g) PST Equipment with Synchrotron Radiation

This method adopts a two-dimensional crystal collimating system, as schematically shown in Figure 7. X-rays diffracted along a particular azimuthal angular range from a specimen are resolved spatially by crystal collimators M_1 and M_2 made of perfect silicon or germanium crystals. The rotation axis of the collimator M_1 is placed parallel to the polarization direction of the synchrotron radiation. The reflection by the second crystal M_2 is perpendicular to that of the first crystal M_1. The two collimators ensure a fixed geometrical correspondence between the specimen and the image on the emulsion film. Momochromatized X-rays are essential as incident beam, because a white incident beam would produce too much unwanted scattered radiation from the polycrystalline specimen. In our experiment without the monochromator C, which was made at HASY LAB, Hamburg, in 1981, such strong undesirable scattering hindered us to detect the wanted X-rays from a specimen because of too low signal/noise ratio. The monochromator C contributes to reducing the background. The obtainable resolution depends mainly on the distance between the specimen SP and the emulsion film F. For the case of a low order reflection from silicon as collimators the angular divergence of the incident and reflected beams of the collimators are of the order of 10^{-5} rad. When the optical path between the film F and the specimen SP is 300 mm, we attain a resolution of 3 μm (300×10^{-5} mm). This value is of the same order as that of the conventional X-ray diffraction topography or X-ray radiography. It may be quite feasible to employ a position sensitive proportional counter as the electronic imaging system. A two-dimensional counter itself has a relatively poor resolution (up to several ten μm). The

resolution obtained at the final stage, however, can be improved by employing asymmetric reflections at the collimators M_1 and M_2, because they produce enlarged PST images, as can be seen from Figure 7.

3. Observation

3.1. Existence of Texture Distribution in a Rolled Aluminium Sheet

Figure 8 (a) represents the 111 reflection Debye-Scherrer ring of a commercially used aluminium plate with a thickness of 0.8 mm. The inhomogeneous intensity distribution characterizes the rolling texture. The azimuthal angle of a place on the reflection ring is indicated by an angle φ measured clockwise from a reference line in Figure 8 (a). Figure 8 (b) represents the PST image observed with the 111 reflected X-rays along a direction of the azimuth angle 90° by means of the Soller slit oscillating technique. An arrow in the topograph indicates the reflection vector. The experimental conditions were MoKα, 40 kV/20 mA, 75 h exposure. The topograph and Debye-Scherrer photograph are positive prints, i.e. white regions are higher radiation areas. The topograph reveals light and dark pattern parallel to the rolling direction. This means that the plastic deformation is not homogeneous along a line perpendicular to the rolling direction. Such lineage structure is schematically depicted in Figure 8 (c). The spatial period of texture irregularity is found to be approximately 1 mm. The internal structure causes a difference between the mechanical properties parallel and normal to the rolling direction. The investigation on a relationship between such texture inhomogeneity and mechanical properties is in progress.

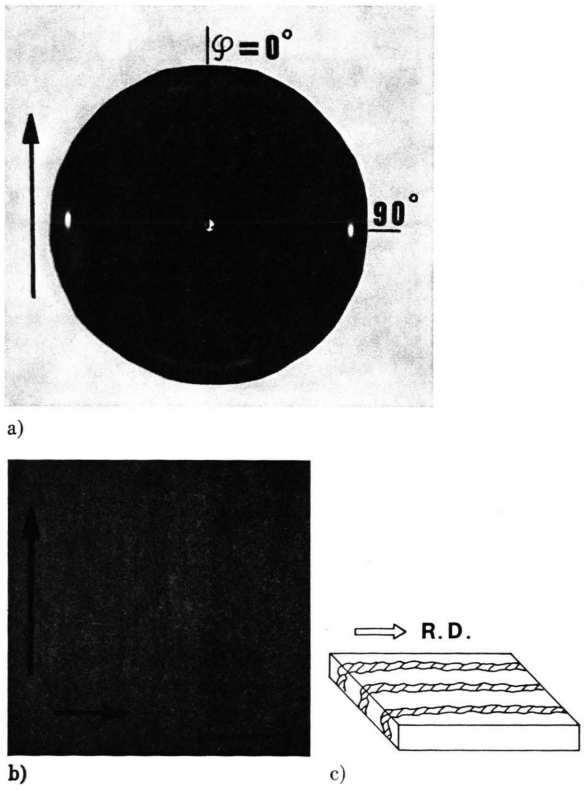

Fig. 8. PST observation of a commercially used aluminium sheet with a thickness of 0.8 mm. The direction of observation is represented by the azimuthal angle φ indicated in (a), the Debye-Scherrer ring of the 111 reflection. (b) PST image at $\varphi = 90°$. Long arrow: rolling direction: short arrow: reflection vector; scale 3 mm. X-ray condition: see text. (c) Schematic presentation of the internal structure due to texture distribution. R.D.: rolling direction.

3.2. Annual Rings of Wood (Japan Cedar)

As an example of observation, Fig. 9 (a) represents a PST image of a Japan cedar observed at the scattering angle 10.8° with the X-Y scanning method under X-ray condition 40 kV/17 mA (MoKα), 20 min exposure. The incident pencil beam has 0.5 mm in diameter. With the diffraction geometry (Fig. 9 (b)), the annual rings of the wood are found to produce strong intensity of the scattered beam. When tilting the specimen (shown by dashed lines in Fig. 9 (b)) under the same diffraction condition fine structures of the annual ring layers are revealed in the PST image, represented in Figure 9 (c). The intensity distribution in the PST image indicates directly the distribution of the material with a structure which yields a peak at the scattering angle 10.8°. The quantitative analysis of these observations should be performed with a knowledge of wood. This kind of PST observation may enable us to interprete the origin and mechanism of kinking or branching.

4. Discussion of the Perspective Fields of Application

Since any kind of scattered X-rays may contribute to the PST images, we have to consider which kind of scattering (diffraction in many cases) is the main factor in the image formation. This consideration and the preliminary experiments (Sect. 3) help us to deduce a feasibility study of the PST application.

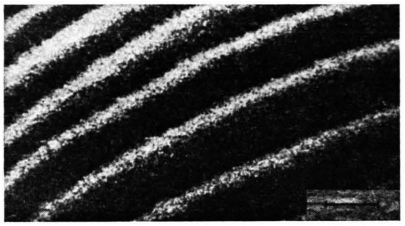

a)

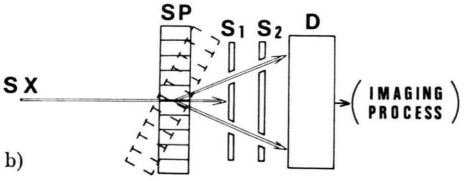

b)

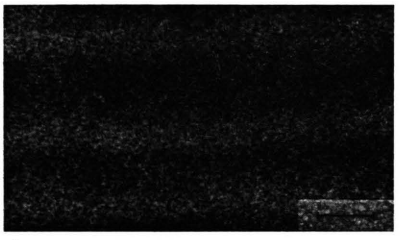

c)

Fig. 9. PST observation of wood (a Japan cedar) by means of the X-Y scanning method. (a) PST image at normal position. White regions with intense radiation correspond to the annual rings. (b) Diffraction geometry for taking the topographs (a) (SP, solid line) and (c) (SP, dashed line). (c) PST image after tilting the specimen by about 30°. Broad white contrast indicates internal structure of the annual ring layers. X-ray condition, see text. Scale mark: 5 mm.

(a) Texture

Texture means, roughly speaking, preferred oriented structure. Such orientation distribution in aluminium plates was the first object observed by the Soller slit oscillating method. The result reveals that the texture distribution exists. Commercially used aluminium plates have a special lineage structure due to texture elongated along the rolling direction. The inhomogeneous texture may cause the difference of mechanical properties along directions parallel and perpendicular to the rolling direction. From the experimental fact we conclude that materials having texture should be characterized by the over-all texture, which is represented with a pole figure [7], and the texture topographs.

(b) Crystallite Size

When the number of repeat units becomes less than about 1000, the width of the diffraction maximum begins to get measurably larger. If $\beta = 2\Delta\theta$ (the increase in the width of the diffraction peak) then

$$\beta = \lambda / t \cos\theta , \tag{1}$$

where t: linear dimension of the crystallites,

λ: wave length and θ: Bragg angle.

For a mosaic block of 0.1 μm and CuKα radiation

$$\beta \sim 1.5 \times 10^{-4} / \cos\theta \quad \text{rad.}$$

At $\theta = 85°$, this gives a spread of the order of

$$1.7 \times 10^{-3} \quad \text{rad.}$$

Therefore this effect should give good contrast in the PST images in cases where the crystallite size of the specimen is locally different.

(c) Strain

Often strain in a specimen, especially if due to cold working, is non-homogeneous, and alters the lattice size in different ways in different crystallites and in different directions in the same crystallite. The reciprocal points are distributed over volumes around the average position. The effect is expressed as

$$\beta = 2\Delta\theta = 2(\Delta d/d)\tan\theta , \tag{2}$$

where d: interplanar spacing.

The strain effect gives sufficient contrast in the PST image if the specimen has locally deformed regions such as "Lüders Band". Certain alloys exhibit a tendency to develop "Lüders lines" or flow lines on the surface when stretched [7]. Such propagation of the Lüders band is a good object to be observed by means of the PST. Inhomogeneous solid solution also alters the crystal lattice and reciprocal lattice size in the same way as strain.

(d) Structure Factor

According to the kinematical theory of diffraction the intensity I_{hkl} of scattered X-rays is proportional to the square of the structure factor F_{hkl} of the specimen:

$$I_{hkl} \propto |F_{hkl}|^2 ,$$

$$F_{hkl} = \sum_n f_n \exp 2\pi i (\boldsymbol{r}_n \cdot \boldsymbol{g}) , \tag{3}$$

$\boldsymbol{g} = (hkl)$: reflection index,

$\boldsymbol{r}_n = (x_n y_n z_n)$: position of n-th atom in the unit cell,

f_n: scattering factor of n-th atom in the unit cell.

Phase transformation is quite a feasible object by using structure factor contrast. Consider a disor-

dered structure which has started the process of ordering to form a superlattice, without altering the size of the parent lattice. All reflections which are common to both structures will be generally sharp, but the additional reflections which the new phase alone produces (supperlattice reflections) will arise only from the small nuclei of ordered phase, and at the same time, show small crystallite size broadening. In a case where the transformation is locally nucleated and then gradually performed all over the specimen, the process can be observed by the PST.

(e) Stress Distribution

The X-ray method of stress determination is based on the measuring of differences in the interplanar spacing of a given set of crystal planes which are variously oriented to the specimen surface [8]. The lattice spacing has to be measured with an error less than the order of 10^{-4} [9]. The PST technique using synchrotron radiation described in the Section 2.2 (g) and in Fig. 7 enables us to determine a distribution of the interplanar spacing precisely enough. For the stress measurement with the PST technique we employ an energy dispersive system, as schematically shown in Figure 10. In this geometry the specimen is fixed at the Bragg angle θ. From Bragg's law the relative error in measuring the interplanar spacing d is given as

$$\Delta d/d = \Delta\lambda/\lambda - \cot\theta \cdot \Delta\theta\,, \qquad (4)$$

where $\Delta\lambda$: deviation of the wave length λ,
Δd: change of the interplanar spacing d,
$\Delta\theta$: error of the measured value θ.

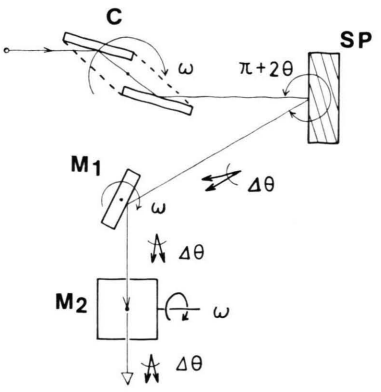

Fig. 10. Schematic principle of stress measurement by means of the energy dispersive system of a PST, in which synchrotron radiation with white spectrum is used. The specimen is fixed at a proper position. $\Delta\theta$: angular divergence of the incident and outgoing beams for the collimators M_1 and M_2. From the rotation angle ω a value of the wave length deviation $\Delta\lambda$ of the beam diffracted from the specimen can be calculated.

The error of $\Delta\theta$ is equivalent to the angular divergence of the incoming or outgoing beams of the collimators M_1 and M_2, the order of which is 10^{-5} (in the case of silicon 220 reflection of MoKα_1, $\Delta\theta \sim 1.1 \times 10^{-5}$). The first term $\Delta\lambda/\lambda$ of Eq. (4) is determined by measuring the rotation angle ω. The accuracy is given for the relevant reflection, independent of the wave length (5.6×10^{-5} for silicon 220 reflection) [10]. Accordingly, in the reflection case ($\theta > 45°$), we attain the order of 10^{-5} as the relative error. The PST with synchrotron radiation provides us a peerless method for observing the stress distribution in the surface of a specimen.

[1] T. Horiuchi and Y. Yoneda, Proceedings of the 32nd Annual Conference of Applied Physics, Japan **1971**, p. 343. Y. Yoneda and Y. Chikaura, KEK-79-34 (1979), p. 85. Proceedings of the plan Meetings on X-ray Instrumentation for Photon Factory, Tsukuba 1979; edited by M. Ando and A. Amemiya, National Laboratory for High-Energy Physics, Japan.
[2] Y. Chikaura, Y. Yoneda, and G. Hildebrandt, J. Appl. Cryst. **15** (1982), in press.
[3] Y. Yoneda and Y. Chikaura, Japan J. Appl. Phys. **21**, 31 (1982).
[4] E. Born, Kristall und Technik **14**, 325 (1979).
[5] E. Born and H. Schwarzbauer, Kristall und Technik **15**, 837 (1980).
[6] Y. Yoneda, T. Horiuchi, and N. Hiramatsu, Japan J. Appl. Phys. **19**, 353 (1980).
[7] B. Chalmers, Physical Metallurgy, Chapt. 5, pp. 157, J. Wiley & Sons, New York 1959.
[8] C. S. Barrett and T. B. Massalski, Structure of Metals, third edition, Chapt. 17, pp. 466–485, McGraw-Hill, New York 1966.
[9] P. Doig, D. Lonsdale, and P. E. J. Flewitt, J. Appl. Cryst. **14**, 124 (1981).
[10] J. H. Beaumont and M. Hart, J. Phys. (E) **7**, 823 (1974).